Cognitive Perception as a Base Model of the Feeling Artificial Intelligence

Anatolii Kargin[a], Tetyana Petrenko[a]

[a] *Ukrainian State University of Railway Transport, Feuerbach sq., 7, Kharkiv, 61050, Ukraine*

Abstract

The need for more advanced Unmanned Systems (US) is supported by the development trends of world society. Artificial Intelligence (AI) plays an important role in maintaining the required level of US autonomy. AI-enabled US developers are focusing on the creation of the third generation of AI namely Feeling AI (FAI) for Autonomous Intelligent US (AIUS). One of the components of the FAI is a Cognitive Perception (CP) model, which overcomes the gap between the two paradigms "data from sensors" and "natural words", which was and is the main problem for the deployment of AIUS. The CP model considered in the work takes into account such cognitive processes as the mapping of data from sensors in iconic memory and its further processing in short-term memory by generalizing and abstracting in order to distill the sense of sensor data and represent it in the form of concepts. An important feature of cognitive perception is the sustainable aging of information and its forgetting over time. The article considers an algorithm that implements a model of cognitive perception with an aging mechanism. The results of computer experiments in which a wheeled warehouse robot was used as an AIUS showed that by adjusting the aging rate coefficients included in the CP model in accordance with the dynamic characteristics of the environment, it is possible to minimize the risks of violating the autonomy of the AIUS when making decisions in conditions of incomplete information.

Keywords

Autonomous intelligent unmanned system, feeling artificial intelligence, cognitive perception, data from sensor, aging of information

1. Introduction

Today, in everyday life, people widely use the services of the Internet of Things and autonomous US with AI [1-3]. The need for more advanced US is supported by the development trends of world society. The military domain, smart cities and smart machines, industrial USs that free a person from performing routine operations or functions in conditions dangerous to life and health, generate a growing demand for intelligent US [1, 4]. Despite significant progress in the field of US creation [5, 6], ensuring the necessary level of their autonomy remains an actual task [7]. AI plays an important role in solving this task. Today, new AI models are in demand, which are specially developed and adapted for the new generation of AIUS [6, 8, 9]. The scientific community is discussing the possibility of creating a general AI for the third generation for AIUS, which takes into account the features of US and has cognitive abilities that support autonomous decision-making in conditions of uncertainty and in an unfriendly environment [10, 11]. The design of the model and blueprint of FAI are proposed [7, 11, 12]. One of the main components of the FAI architecture is the perception system, which implements such a cognitive function as the distillation of the sense of data from sensors [7]. The FAI architecture proposed in [7] shown in Figure 1. Four Knowledge Bases (KBs) are shown by circle tags. AIUS functions are implemented by nine FAI Engines. They are shown as hexagon tags. Their connections are done that show from which KB the engine uses knowledge. The perception engine of CP model

ICST-2023: Information Control Systems & Technologies, September 21-23, 2023, Odesa, Ukraine.
EMAIL: kargin@kart.edu.ua (A. Kargin); petrenko_tg@kart.edu.ua (T. Petrenko)
ORCID: 0000-0003-2885-9071 (A. Kargin); 0000-0001-6305-7918 (T. Petrenko)

uses KB “What Is This”. The rest of the components of FAI architecture are used for decision-making and control. This article is devoted to the discussion of the model that is the basis of the CP system. The model of knowledge representation in the KB “What Is This” (Figure 1), the CP algorithm which distilling the sense of the data from sensors are discussed. Also, the results of computer experiments on the effect of the aging of data from sensors on the assessment of the meaning of situation are done.

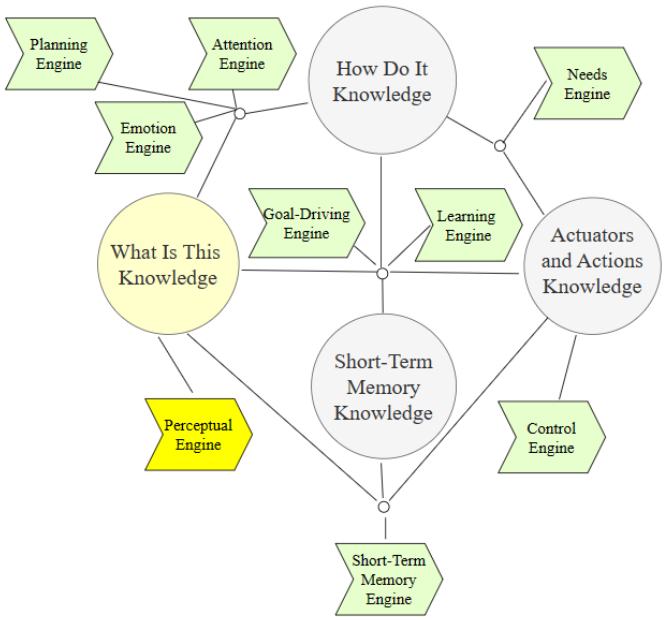

Figure 1: FAI architecture blueprint

2. Problem Discussion

Work [7] shows that the arsenal of AI approaches and models that can be adapted to solve the problem of cognitive perception by distilling the meaning of data from AIUS sensors can be divided into two groups: 1) oriented to processing data from sensors and 2) oriented to knowledge processing. The first group includes approaches of data from sensors fusion (intelligent analysis, extraction of knowledge from data streams, aggregation of disparate data [13, 14]). These models can be used at the stages of primary data processing, but they do not solve the problem of obtaining the meaning of a spatio-temporal data set from sensors. For the same reason, it is difficult to use "pure" models of artificial neural networks for applications to which AIUS belongs. AI models of another group, focused on knowledge processing including the distillation of knowledge represented in symbolic form [15], are capable to present the meaning of situation. In this case, the meaning is given by the concepts expressed by the words of natural language. A CP as FAI component overcomes this gap between the two paradigms "data from sensors" and "natural words", which was and is the main challenge for the deployment of AIUS.

The knowledge-based AI approach, known as rule-based systems [16], allows the implementation of decision-making tasks, taking into account most of the above-mentioned features of US. Decision-making in robotics, Internet of Things, smart machines is carried out on the rule-based inference engine [17]. They are widely used in embedded real-time systems, however, the problem of obtaining a meaning of the situation presented by data from sensors and giving it in a generalized form by concepts remains relevant. On the basis of the above analysis, in [12] it is proposed to solve the problem of distilling the meaning of data from sensors based on the approach of granular calculations and the conceptual model of L. Zadeh “Computing with Words” [18]. The information processing scheme in the CP system of AIUS using this approach is as follows. Data from the sensors are granulated after pre-processing. At the output of the granulation block, the data is presented on the set of all granules with fuzzy characteristics. Next, the data sense distillation block performs generalization and abstraction of data based on domain knowledge presented verbally by experts in the form of natural

language word meanings. At the output of the distillation unit there are estimates of the data set, in the form of a small number of numerous fuzzy characteristics of the meaning of the whole situation. Further, the fuzzy characteristics of the meaning of the situation are used as input numerical variables of algorithms of the fuzzy logic systems in AIUS. At the output of this unit, the numerical values of the control signals are transmitted to the actuators of the AIUS and are implemented by various controllers.

The CP model takes into account the main features of wildlife perception systems. First, at each moment of time, the meaning is calculated not of the complete situation, but of some fragment of the AIUS environment, allocated by the attention mechanism. The meaning of the complete situation is formed sequentially by moving attention from one fragment of the environment to another. Secondly, a sequentially formed description of the meaning of the complete situation is supported by else one cognitive mechanism of data aging. Thanks to this mechanism, the confidence that the calculated meaning of the situation corresponds to the real situation at the current time is formed taking into account the fact that the meaning of individual fragments was calculated earlier at different points in time. For the real conditions in which AIUS operates, it is especially important to take into account the dynamic characteristics of the environment in order to minimize the risks from the decisions made. If data aging is not taken into account, then the meaning of the complete situation, formed by a sequence of fragments, the meaning of which was calculated on the basis of data obtained long before the current time, may not correspond to reality at all. Thirdly, AIUS requires the dynamic control model with data aging mechanism. Decisions that are made only on the basis of current data are associated with no less risks. Static control models, in which the history of changes in the state of the environment and their dynamic characteristics are not taken into account, cannot support the autonomous functioning of AIUS in real conditions.

This article examines the CP algorithm of distilling the meaning of data from sensors which takes into account above two cognitive mechanisms, namely attention and data aging.

Before proceeding to the consideration of the algorithm for distilling the meaning of data from sensors in the CP system, the results of which demonstrate a significant reduction in the dimensionality of the AIUS control tasks, we will introduce basic definitions [12, 19].

3. A model of cognitive perception of data from sensors

A FAI elementary portion of knowledge about the environment of AIUS is the Knowledge Granule (KG). Such a portion of knowledge has an External Meaning of KG (EMKG) and an Internal Meaning of KG (IMKG) in FAI [19].

3.1. External meaning of KG

The formal definition of EMKG is as follows

$$< N, know, \{< M_i, (a_i, b_i, v_i, g_i) >, \forall M_i \in \Omega_N\} > \quad (1)$$

where N is the identifier of the KG; *know* is an sign model of N KG; $\Omega_N = \{M_i, i=1, 2,...,I\}$ is set of KGs used to reveal the meaning of the N granule; M_i is the identifier of the KG of lower level of abstraction.

Definition (1) specifies the parameters that are numerically evaluated: $-1 \le a_i \le +1$ - is the expert's certainty that the concept M_i must be present ($a_i = +1$) in the definition to reveal the meaning of concept of N or absent ($a_i = -1$); b_i is time delay when determining dynamic relations; v_i is speed of aging of information regarding M_i; g_i is informational completeness, which determines whether there is enough knowledge about the KG of M_i to understand the meaning of the KG of N.

In the KB of FAI, the set of KGs is structured, the granules are arranged according to the levels of abstraction and includes the set of KGs: $\Omega_{KG} = \Omega^0_{KG} \cup \Omega^1_{KG} \ldots \Omega^i_{KG} \ldots \cup \Omega^k_{KG}$, where Ω^i_{KG} is a subset of KGs of the ith level [17, 19]. The levels are localized according with types of restriction noted in L. Zadeh Restriction-Centered Theory [20]. There are three types of restriction:

1) Restriction by quantitative abstraction. This is the sensors data granulating based on restrictions on the accuracy of the solution.

2) Restriction by definitive abstraction. This is a mapping of a data quantitative constraint presented by data from sensors granules into a word semantic constraint presented by KGs.

3) Restriction by generalizing abstraction. This is a mapping sense of words of lower level of abstraction into sense of words of upper level of abstraction.

In this article two first types of restriction (quantitative and definitive abstractions) are combined at zero level. KG of zero level is presented by word and sense this word determines the external meaning data from sensor. Figure 2.a shows the representation of the EMKG of the one granule in the general case using the certainty factor function [19] which is given by a piecewise linear function with six parameters: a, b, c, d, e, f. In Figure 2.b shows an example of granulation of data from a distance sensor and representation of these data of the EMKGs of KGs. This sensory modality is represented by four granules that describe knowledge about a moving object-obstacle, which can be located either in the 1st sector, or in the 2nd, or in the 3rd, or there is a situation when there is no one within the reach of the sensor.

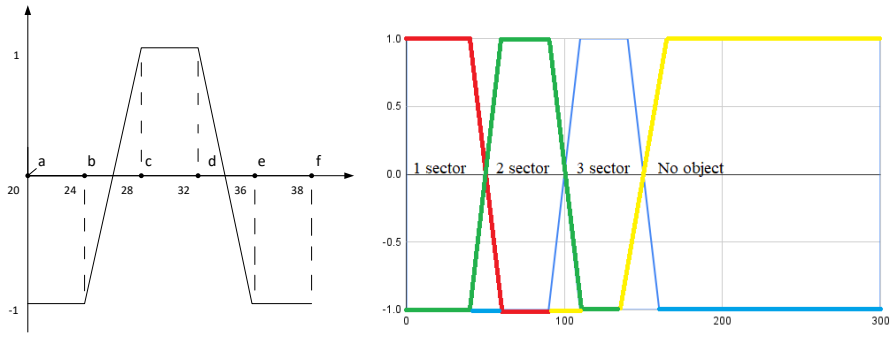

а) б)

Figure 2: Graphical illustration of the determination of the zero-level EMKG: a) general view of the of the certainty factor function for one granule; b) an example of the definition of the EMKG modality of localization of objects around the robot

The knowledge presentation in the form (1) will be illustrated using the example of a warehouse robot (co-bot [21]), namely a fragment of knowledge required for safe crossing of an unregulated intersection to continue moving along a given warehouse route. Figure 3 shows the situation when the co-bot on the entrance road of the intersection sequentially scans three other access roads in order to assess the situation (dangerous or safe to perform a maneuver at the intersection).

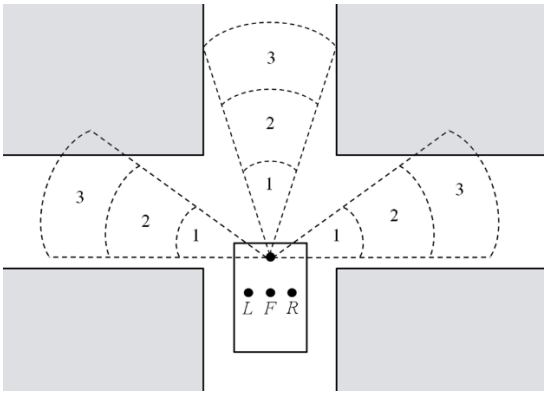

Figure 3: An example of co-bot scanning situations at a crossroads

In Figure 4 shows a fragment of the KB that defines the situation at the crossroads (Figure 3). Modeling and experiments were carried out with the co-bot prototype, the hardware of which is based on robot with a four-wheel drive Multi Chassis-4WD Robot Kit ATV chassis, Arduino Mega microcontroller, ESP8266 microcontroller and Motor shield kit.

1. <***3.EverywhereSafe***, *Everywhere safe*, {<***2.RSafe***,(0.75,*t*,0.1,0.33)>, <***2.LSafe***,(0.75,*t*,0.1,0.33)>, <***2.FSafe***,(0.75,*t*,0.1,0.33)>};

2. <***3. EverywhereDangerous***, *Everywhere dangerous*, {<***2.FDirecDang***, (0.75, *t*, 0.1, 1.0)>, <***2.LDirecDang***, (0.75, *t*, 0.1, 1.0)>, ***2.RDirecDang***, (0.75, *t*, 0.1, 1.0)>}>;
3 <***2.FSafe***, *Forward safe*, {<***1.FSafe1*** (0.75, *t*, 0.1, 1.0)>, ***1.FSafe2*** (0.75, *t*, 0.1, 1.0)>};
4. <***2.LSafe,*** *Left safe*, {<***1.LSafe1*** (0.75, *t*, 0.1, 1.0)>, ***1.LSafe2*** (0.75, *t*, 0.1, 1.0)>};
5. <***2.RSafe,*** *Right safe*, {<***1.RSafe1*** (0.75, *t*, 0.1, 1.0)>, ***1.RSafe2*** (0.75, *t*, 0.1, 1.0)>};
6 <***2.FDang***, *Forward safe*, {<***1.FDirecDang1*** (0.75, *t*, 0.1, 1.0)>, ***1.FDirecDang2*** (0.75, *t*, 0.1, 1.0)>};
7. <***2.LDang,*** *Left safe*, {<***1.LDirecDang1*** (0.75, *t*, 0.1, 1.0)>, ***1.LDirecDang2*** (0.75, *t*, 0.1, 1.0)>};
8. <***2.RDang,*** *Right safe*, {<***1.RDirecDang1*** (0.75, *t*, 0.1, 1.0)>, ***1.RDirecDang2*** (0.75, *t*, 0.1, 1.0)>};
9. <***1.FSafe1***, *Forward safe 1st-case*, {<***0.ObjectForward*0.Loc&1sector***, (-0.75, *t*, 0.1, 0.33)>, <***0.ObjectForward*0.Loc&2sector***, (-0.75, *t*, 0.1, 0.33)>, <***0.ObjectForward*0.Loc&3sector***, (-0.75, *t*, 0.1, 0.33)>, }>;
10. <***1.LSafe1,*** *Left safe 1st-case*, {<***0.ObjectLeft*0.Loc&1sector***, (-0.75, *t*, 0.1, 0.33)>, <***0.ObjectLeft*0.Loc&2sector***, (-0.75, *t*, 0.1, 0.33)>, <***0.ObjectLeft*0.Loc&3sector***, (0.75, *t*, 0.1, 0.33)>}>;
11. <***1.RSafe1,*** *Right safe 1st-case*, {<***0.ObjectRight*0.Loc&1sector***, (-0.75, *t*, 0.1, 0.33)>, <***0.ObjectRight*0.Loc&2sector***, (-0.75, *t*, 0.1, 0.33)>, <***0.ObjectRight*0.Loc&3sector***, (-0.75, *t*, 0.1, 0.33)>}>;
12. <***1.FSafe2***, *Forward safe 2st-case*, {<***0.ObjectForward*0.DirMov&removed***, (0.75, *t*, 0.1, 1.0)>};
13. <***1.LSafe2,*** *Left safe 2st-case*, {<***0.ObjectLeft*0.DirMov&removed***, (0.75, *t*, 0.1, 1.0)>};
14. <***1.RSafe2,*** *Right safe 2st-case*, {<***0.ObjectRigh*0.DirMov&removed***, (0.75, *t*, 0.1, 1.0)>};
15. <***1.FDirecAlmSafe***, *Forward direction almost safe*, {<***0.ObjectForward*0.Loc&1sector***, (-0.75, *t*, 0.1, 0.2)>, <***0.ObjectForward*0.Loc&2sector***, (-0.75, *t*, 0.1, 0.2)>, <***0.ObjectForward*0.Loc&3sector***, (0.75, *t*, 0.1, 0.2)>, <***0.ObjectForward*0.DirMov&approached***,(0.75,*t*, 0.1, 0.2)>, <***0.ObjectForward*0.Speed&slow***, (0.75, *t*, 0.1, 0.2)>}>;
16. <***1.LDirecAlmSafe***, *Left direction almost safe*, {<***0.ObjectLeft*0.Loc&1sector***, (-0.75, *t*, 0.1, 0.2)>, <***0.ObjectLeft*0.Loc&2sector***, (-0.75, *t*, 0.1, 0.2)>, <***0.ObjectLeft*0.Loc&3sector***, (0.75, *t*, 0.1, 0.2)>, <***0.ObjectLeft*0.DirMov&approached***, (0.75, *t*, 0.1, 0.2)>, <***0.ObjectLeft*0.Speed&slow***, (0.75, *t*, 0.1, 0.2)>}>;
17. <***1.RDirecAlmSafe***, *Right direction almost safe*, {<***0.ObjectRight*0.Loc&1sector***, (-0.75, *t*, 0.1, 0.2)>, <***0.ObjectRight*0.Loc&2sector***, (-0.75, *t*, 0.1, 0.2)>, <***0.ObjectRight*0.Loc&3sector***, (0.75, *t*, 0.1, 0.2)>, <***0.ObjectRight*0.DirMov&approached***, (0.75, *t*, 0.1, 0.2)>, <***0.ObjectRight*0.Speed&slow***, (0.75, *t*, 0.1, 0.2)>}>;
18. <***1.FDirecAlmDang,*** *Forward direction almost dangerous*, {<***0.ObjectForward*0.Loc&1sector***, (-0.75, *t*, 0.1, 0.25)>, <***0.ObjectForward*0.Loc&2sector***, (0.75, *t*, 0.1, 0.25)>, <***0.ObjectForward*0.DirMov&approached***, (0.75, *t*, 0.1, 0.25)>, <***0.ObjectForward*0.Speed&slow***, (0.75, *t*, 0.1, 0.25)>}>;
19. <***1.LDirecAlmDang,*** *Left direction almost dangerous*, {<***0.ObjectLeft*0.Loc&1sector***, (-0.75, *t*, 0.1, 0.25)>, <***0.ObjectLeft*0.Loc&2sector***, (0.75, *t*, 0.1, 0.25)>, <***0.ObjectLeft*0.DirMov&approached***, (0.75, *t*, 0.1, 0.25)>, <***0.ObjectForward*0.Speed&slow***, (0.75, *t*, 0.1, 0.25)>}>;
20. <***1.RDirecAlmDang,*** *Right direction almost dangerous*, {<***0.ObjectRight*0.Loc&1sector***, (-0.75, *t*, 0.1, 0.25)>, <***0.ObjectRight*0.Loc&2sector***, (0.75, *t*, 0.1, 0.25)>, <***0.ObjectRight*0.DirMov&approached***, (0.75, *t*, 0.1, 0.25)>, <***0.ObjectRight*0.Speed&slow***, (0.75, *t*, 0.1, 0.25)>}>;
21. <***1.FDirecDang1,*** *Forward direction dangerous 1st*, {<***0.ObjectForward*0.Loc&1sector***, (-0.75, *t*, 0.1, 0.25)>, <***0.ObjectForward*0.Loc&2sector***, (0.75, *t*, 0.1, 0.25)>, <***0.ObjectForward*0.DirMov&approached***, (0.75, *t*, 0.1, 0.25)>, <***0.ObjectForward*0.Speed&fast***, (0.75, *t*, 0.1, 0.25)>}>;
22. <***1.LDirecDang1,*** *Left direction dangerous 1st*, {<***0.ObjectLeft*0.Loc&1sector***, (-0.75, *t*, 0.1, 0.25)>, <***0.ObjectLeft*0.Loc&2sector***, (0.75, *t*, 0.1, 0.25)>, <***0.ObjectLeft*0.DirMov&approached***, (0.75, *t*, 0.1, 0.25)>, <***0.ObjectForward*0.Speed&fast***, (0.75, *t*, 0.1, 0.25)>}>;
23. <***1.RDirecDang1,*** *Right direction dangerous 1st-case*, {<***0.ObjectRight*0.Loc&1sector***, (-0.75, *t*, 0.1, 0.25)>, <***0.ObjectRight*0.Loc&2sector***, (0.75, *t*, 0.1, 0.25)>, <***0.ObjectRight*0.DirMov&approached***, (0.75, *t*, 0.1, 0.25)>, <***0.ObjectRight*0.Speed&fast***, (0.75, *t*, 0.1, 0.25)>}>;
24. <***1.FDirecDang2***, *Forward direction dangerous 2st-case* , {<***0.ObjectForward*0.Loc&1sector***, (0.75, *t*, 0.1, 1.0)>}>;
25. <***1.LDirecDang2***, *Left direction dangerous 2st-case*, {<***0.ObjectLeft*0.Loc&1sector***, (0.75, *t*, 0.1, 1.0)>}>;
26. <***1.RDirecDang2***, *Right direction dangerous 2st-case*, {<***0.ObjectRight*0.Loc&1sector***, (0.75, *t*, 0.1, 1.0)>}>;
27. <***0.ObjectRight****, *Object in right allocated by attention*, {<*Event*(***0.Direc***&***right)***>, <***0.Loc***>, <***0.Speed***>, <***0.DirMov***>}>;
28. <***0.ObjectForw****, *Object in forward allocated by attention*, {<*Event*(***0.Direc***&***forw)***>,<***0.Loc***>, <***0.Speed***>, <***0.DirMov***>}>;
29. <***0.ObjectLeft****, *Object in left allocated by attention*, {< *Event*(***0.Direc***&***left)***>,<***0.Loc***>, <***0.Speed***>, <***0.DirMov***>}>;
30. <***0.DirMov***, *direction of movement*,{<***approach***,(*-300,-25,25,300,300,300*)>,<***remove***,(*-300,-300,-300,-25,25, 300*)>}>;
31. <***0.Speed***, *Speed of movement*, {<***stop***, (*0,0,0,0.2,0.4,4.0*)>, <***slow***, (*0,0.5,0.8,1.3,1.5,4.0*)>, <***fast***, (*0,1.3,2.0,4.0,4.0,4.0*)>}>;
32. <***0.Direc***, *Direction of the ultrasonic sensor*, {<***left***, *(-90,-90,-90,-35,-25,90*)>, <***forward***, *(-90,-35,-25,25,35,90*)> <***right***, *(-90, 25, 35, 90, 90 ,90*)>}>;
33. <***0.Loc***, *Object location*, {<***1sector***,*(0,0,0,40,60,300*)>, <***2sector***,*(0,40,60,90,110,300*)>, <***3sector***,*(0,90,110,135,165,300*)>}>.

Figure 4: A fragment of the KB that defines the situation at the crossroads

The CP of co-bot based on following sensors: 10 infrared reflection sensors ky-033 for detecting marks on the floor, an ultrasonic sensor HC-SR04, installed on a rotary platform with a servo drive SG90, and an odometer sensor H206. The situation around the robot is represented by the environment

map built on the basis of data from an ultrasonic sensor on a servo drive that sets the direction and measures the location of the object identified by the sensor. The speed of the moving object-obstacle and its direction of movement are calculated, too. In Figure 3, the model for displaying the current state of the co-bot's environment is proposed in the form of a two-dimensional spatial map. Figure 3 shows a simplified version, when the space covering the sensor is divided into 3 directions. Calculations of the fuzzy characteristics of granules of 0 level were carried out with a model of *18*th sectors with a viewing angle of ±*15* degrees and a sensor distance measurement error of ±5 cm and a rotary platform positioning accuracy of ±*7* degrees. The definition of the meaning of these KGs (Figure 4) is given on their domain scales as shown in Figure 2.b. The granules are distributed by levels of abstraction. The level is indicated by the first digit of the KG identifier, for example, ***0.Speed*** indicates that the speed sensor modality belongs to the *0*th level. This portion of knowledge (Figure 4, line 31) defines EMKG of three KGs in the form of concepts of speed of movement, namely the object-obstacle does not move (***stop***), moves slowly (***slow***) and moves fast (***fast***). The determination of the EMKG of these granules is set on the universe of movement speed in cm/s by the parameters of the certainty factor function, as shown in Figure 2. At the zero level of KB, 11 granules are defined. These are four KGs of the ***0.Loc*** modality with KG identifiers ***1sector***, ***2sector***, ***3sector***, which determine whether the object-obstacle is located in the *1*st, *2*nd, or *3*rd sector; three KGs ***stop***, ***slow***, ***fast*** of ***0.Speed*** modality (movement speed of object-obstacle) and two KGs ***approach***, ***remove*** of ***0.DirMov*** modality, which determine whether the object approaches or moves away from the co-bot and three KGs ***left***, ***forward***, ***right*** of ***0.Direc*** modality. In the definitions of EMKG in Figure 4, the identifiers of the KGs are coupled to the identifiers of the sensory modality to which they belong. For example, the link to the ***fast*** KG of the ***0.Speed*** modality is given in the form ***0.Speed&fast***. In the definition of three structures of the object-obstacle deserves special attention. When the rotary platform is set in a certain position, for example, right+75°, the data obtained characterizes this certain direction. Therefore, they must be "tied" to this value, namely the readings of the ***0.Direc*** modality sensor. The asterisk at the end of the identifier indicates that it is a structure of same level granules. with three modalities (in Fig. 3,). For example, the structure with identifier ***0.ObjectRight**** (27 line in Figure 4) defines 8 KGs of three modalities ***0.Loc***, ***0.Speed***, ***0.DirMov***. The notation ***Event(0.Direc&right)*** means that as soon as an event occurs (the rotating platform will take the *right+75°* position), the attention mechanism will "focus" on this direction and all data received from the sensors of modalities indicated in structure definition are stored in these ***0.Direc&right**** structure.

3.2. Internal meaning of KG

Building models of the "general sense of something" is the main task of such AI branch as artificial general intelligence [22, 23]. Another view on meaning is proposed for FAI CP model [12, 19]. IMKG is a numerical assessment of the degree of correspondence of EMKG (1) with the situation represented by data from sensors. The numerical value of the estimate of the IMKG depends, firstly, on the parameters in (1) of the corresponded EMKG, and secondly, on the IMKGs indicated in (1) and calculated for the same data from the sensors. In other words, the IMKG is an assessment of the correspondence of the parameterized verbal representation of the sense of KG to the data from the sensors, on the basis of which the EMKG is determined. A formal computational model of the IMKG is given [19]. IMKG is quantified based on fuzzy Certainty Factor (CF). In [12], fuzzy CF was introduced as a fuzzy LR number **X** follows

$$\boldsymbol{X}: \{x | m_{\boldsymbol{X}}(x), \forall x \in [-q, +q], q \geq +1\} \tag{2}$$

with a Gaussian L-R membership function [24, 25]

$$\begin{aligned} m_{\boldsymbol{X}}^{L}(x) &= exp(-(x-\alpha)^2/2 \cdot (v_L \cdot t_L)^2), \forall x \in [-1, \alpha] \\ m_{\boldsymbol{X}}^{R}(x) &= exp(-(x-\alpha)^2/2 \cdot (v_R \cdot t_R)^2), \forall x \in (\alpha, +1] \end{aligned} \tag{3}$$

with three parameters: ($-1.0 \le \alpha \le +1.0$) is CF; t_L is the time interval that has passed since the moment of receiving the data; t_R is the time interval that has passed since the data change; v_L and v_R are the normalized aging rates. Time interval t_R is used when impact of data aging on certainty is modelled.

Presumed certainty is a numerical estimate of fuzzy CF that takes into account the aging of data and is calculated on the basis of (2) and (3) by formula (4).

$$cf = \alpha \cdot k_t \tag{4}$$

where $k_t = 1 - \frac{\sum_{\forall x \in [-1,\alpha)} m_X^L(x) + \sum_{\forall x \in (\alpha,+1]} m_X^R(x)}{Card([-1,+1]) - 1}$;

*Card(***X***)* is scalar cardinality of a fuzzy set **X**.

The aging of the data over time leads to the presumed certainty tends to zero and over time to a complete lack of certainty, that is, $cf \approx 0$. For cases when time intervals are small (or from the moment of receiving data, or, in special cases, from the moment of data change), the certainty does not change much compared to α, that is, $cf \approx \alpha$. Thus, the numerical value of the IMKG is fuzzy CF and if needed Presumed CF (PCF).

The FAI CP algorithm for computing IMKG is shown below in Figure 5.

4. Experiments with appliance FAI CP computing algorithm of IMKG

The experiments are devoted to the study the cognitive mechanisms of attention and data aging. The PCF computation of complete situation at the intersection, formed by attention as a sequence of data fragments (Figure 3), obtained at different time before the current time is being considered. The aging of the data received from the AIUS sensors over time and, as a result, of the aging of the IMKG describing the PCF is computed. The case is being considered, when the co-bot drove up the entrance road to the intersection, as shown in Figure 3, stopped to obtain data and build a model of the complete situation at the intersection. Attention mechanism carry out the scanning of the environment by step-by-step positioning from right to left of the rotary platform on which the ultrasonic sensor is installed. According to the technical characteristics of the sensor, the number and sequence of passing the following positions by the rotary platform (in the directions of the sensor's vision) are set: $right^{+75^\circ}$, $right^{+45^\circ}$, $forward^{+15^\circ}$, $forward^{-15^\circ}$, $left^{-45^\circ}$, $right^{-75^\circ}$. Building a situation model of one such fragment (turning the platform from the current position to the next direction, receiving and processing data from the sensor and calculating according to the FAI CP computing algorithm of IMKG) takes 200 ms. When setting up the fuzzy CF model in the considered experiment, 100 ms of real time was taken as a unit of time t_L and t_R in (3). Accordingly, parameter b in (1) is related to the real time of the experiment by ratios of 1:100.

The state of the co-bot's environment (intersection map) at an arbitrary moment of time *t* is represented by IMKG in the form of PCF on the next set of granules:

$$\begin{aligned}
&cf_{right^{+75^\circ}sec\,1}(t), cf_{right^{+75^\circ}sec\,2}(t), cf_{right^{+75^\circ}sec\,3}(t),\\
&cf_{right^{+45^\circ}sec\,1}(t), cf_{right^{+45^\circ}sec\,2}(t), cf_{right^{+45^\circ}sec\,3}(t),\\
&cf_{forward^{+15}sec\,1}(t), cf_{forward^{+15^\circ}sec\,2}(t), cf_{forward^{+15^\circ}sec\,1}(t),\\
&cf_{forward^{-15^\circ}sec\,1}(t), cf_{forward^{-15^\circ}sec\,2}(t), cf_{forward^{-15^\circ}sec\,3}(t),\\
&cf_{left^{-45^\circ}sec\,1}(t), cf_{left^{-45^\circ}sec\,2}(t), cf_{left^{-45^\circ}sec\,3}(t),\\
&cf_{left^{-75^\circ}sec\,1}(t), cf_{left^{-75^\circ}sec\,2}(t), cf_{left^{-75^\circ}sec\,3}(t).
\end{aligned} \tag{5}$$

In (5), for example, $cf_{right^{+75^\circ}sec\,1}(t)$ denotes the PCF that assesses the confidence in the presence of an object-obstacle in the *1*st sector in the *right+75°* direction (Figure 3). In graphic form in Figure 6, not all KG from (5) are given, but only four. The blue color shows the values of $cf_{right^{+75^\circ}sec\,1}$ of KG *right+75°sec1*. Values $cf_{forward^{-15^\circ}sec\,1}$ are shown in red.

Input is data from sensors modality, domain KB in the form of a structure Figure 4, in which the KG is the definition of "What is it" (Figure 1) in the form of prototypes (1).

Output is set of fuzzy CF $(\alpha, t_L, t_R)_{KGil}$, $\forall KG_{il} \in \Omega^l_{KG}$, $\forall \Omega^l_{KG} \in \Omega^0_{KG} \cup \Omega^1_{KG} \ldots \cup \Omega^k_{KG}$

Precalculations of time delays

while $l \le L$, where $l = 1,2,\ldots,L$, L is quantity of levels of KB **do**

while $n \le N$, where $n = 1,2,\ldots,N$, N is quantity of KG of lth levels **do**

$t^{ln}_L = t^{ln}_L + 1$; $t^{ln}_R = t^{ln}_R + 1$;

end while

end while

if data from the sensor was not received **then goto end** IMKG

Step 1. Quantitative and Definitive Abstraction

while $j \le J$, where J is quantity of modality sensors **do**

get x^* data from sensor j

while $h \le H$, where H is quantity of sensor IGs **do**

Calculate fuzzy CF:

$$\alpha_{jh} = \begin{cases} -1.0, & if\ x^* \in [a_{jh}, b_{jh})\ \text{ or }\ x^* \in [e_{jh}, f_{jh}] \\ -1.0 + 2\dfrac{x^* - b_{jh}}{c_{jh} - b_{jh}}, & if\ x^* \in [b_{jh}, c_{jh}) \\ +1.0 - 2\dfrac{x^* - d_{jh}}{e_{jh} - d_{jh}}, & if\ x^* \in [d_{jh}, e_{jh}) \\ +1.0, & if\ x^* \in [c_{jh}, d_{jh}) \end{cases}$$

end while

end while

Step 2. Generalizing Abstraction

while $l \le L$, where $l = 1,2,\ldots,L$, L is quantity of levels of KB **do**

while $n \le N$, where $n = 1,2,\ldots,N$, N is quantity of KG of lth levels **do**

Calculate fuzzy CF of KG_{ln}

α_{ln}

$t^{ln}_L = 0$

$$t^{ln}_R = \begin{cases} 0, & if\ (\alpha_{ln} \ge \varepsilon\ \ \&\ \ \bar{}q_{ln} = 0)\ or\ (\alpha_{ln} \le -\varepsilon\ \ \&\ \ \bar{}q_{ln} = 1) \\ \bar{}t^{ln}_R, & atherwise \end{cases}$$

$$q_{ln} = \begin{cases} 1, & if\ (\alpha_{ln} \ge \varepsilon\ \ \&\ \ \bar{}q_{ln} = 0) \\ 0, & if\ (\alpha_{ln} \le -\varepsilon\ \ \&\ \ \bar{}q_{ln} = 1) \\ \bar{}q_{ln}, & otherwise \end{cases}$$

end while

end while

Figure 5: FAI CP computing algorithm of IMKG

Yellow and green colors show the values of presumed certainty of $cf_{left^{-75^\circ} sec\,3}$ and $cf_{left^{-75^\circ} sec\,2}$, respectively. On the column charts in Figure 6, the value of PCF (4) is indicated on the ordinate axis, and time on the scale of 1:100 ms is indicated on the abscissa axis. The following time fragment is given for the *7*th moments of time *t*.

$$\begin{aligned}
&t = 2, right^{+75^\circ}: cf_{right^{+75^\circ} sec\,1} = -0.94, cf_{forward^{-15^\circ} sec\,1} = 0, cf_{left^{-75^\circ} sec\,2} = 0, cf_{left^{-75^\circ} sec\,3} = 0 \\
&t = 4, right^{+45^\circ}: cf_{right^{+75^\circ} sec\,1} = -0.16, cf_{forward^{-15^\circ} sec\,1} = 0, cf_{left^{-75^\circ} sec\,2} = 0, cf_{left^{-75^\circ} sec\,3} = 0 \\
&t = 12, left^{-75^\circ}: cf_{right^{+75^\circ} sec\,1} = -0.01, cf_{forward^{-15^\circ} sec\,1} = -0.05, cf_{left^{-75^\circ} sec\,2} = -0.94, cf_{left^{-75^\circ} sec\,3} = 0.94 \\
&t = 14, right^{+75^\circ}: cf_{right^{+75^\circ} sec\,1} = -0.02, cf_{forward^{-15^\circ} sec\,1} = -0.02, cf_{left^{-75^\circ} sec\,2} = 0.16, cf_{left^{-75^\circ} sec\,3} = -0.16 \\
&t = 16, right^{+45^\circ}: cf_{right^{+75^\circ} sec\,1} = -0.003, cf_{forward^{-15^\circ} sec\,1} = 0.02, cf_{left^{-75^\circ} sec\,2} = -0.05, cf_{left^{-75^\circ} sec\,3} = 0.05 \\
&t = 18, forward^{+15^\circ}: cf_{right^{+75^\circ} sec\,1} = 0.003, cf_{forward^{-15^\circ} sec\,1} = 0.007, cf_{left^{-75^\circ} sec\,2} = -0.02, cf_{left^{-75^\circ} sec\,3} = 0.02 \\
&t = 24, left^{-75^\circ}: cf_{right^{+45^\circ} sec\,1} = -0.002, cf_{forward^{-15^\circ} sec\,1} = -0.003, \\
&\qquad cf_{left^{-75^\circ} sec\,2} = 0.94, cf_{left^{-75^\circ} sec\,3} - 0.94
\end{aligned} \tag{6}$$

In (6), each line contains data for a separate time moment. So, for example, the second line shows the data for time *t=4*, when the rotary platform is positioned in the *right45°* direction and contains the presumed certainty values of four KGs at this time: $cf_{right^{+75^\circ}sec\,1}, cf_{forward^{-15^\circ}sec\,1}, cf_{left^{-75^\circ}sec\,2}, cf_{left^{-75^\circ}sec\,3}$. Since the data of the *right75°* direction were obtained earlier by two units of time, the presumed certainty of the granule *right75°sec1* according to (4) was calculated taking into account aging at *t=2* units of time. The presumed certainty of the last three KGs was calculated on the basis of very old data, since data from these directions had not yet been received. Therefore, the value of their presumed certainty is *cf=0*, there is complete uncertainty about the presence or absence of an object-obstacle in these sectors. IMKG in the form of presumed certainty in (6) are calculated for the largest value of the data aging rate coefficient $v_L=v_R=1$. Therefore, the presumed certainty of the *right75°sec1* KG, the value of which was obtained at the previous monitoring step, approaches zero $cf_{right^{+75^\circ}sec\,1} = -0.16$, despite the fact that two time units earlier (200 ms) it was equal to $cf_{right^{+75^\circ}sec\,1} = -0.94$.

In Figure 6 shows the results of the calculation of the IMKG of the same KG for the same time fragment for different data aging rate coefficients.

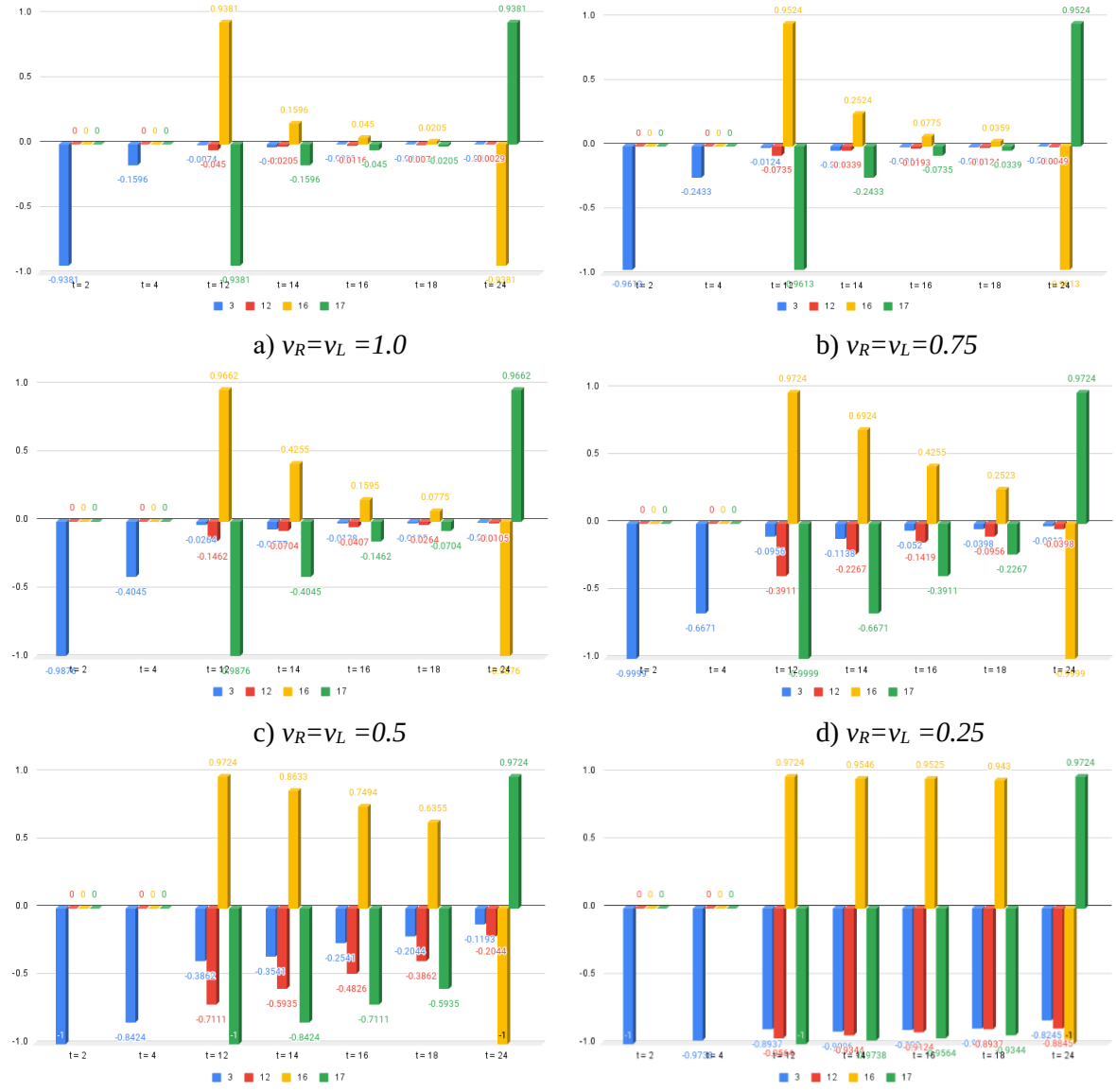

a) $v_R=v_L=1.0$ b) $v_R=v_L=0.75$

c) $v_R=v_L=0.5$ d) $v_R=v_L=0.25$

i) $v_R=v_L=0.1$ g) $v_R=v_L=0.01$

Figure 6: Dependence of the PCF of IMKG on the data aging speed coefficient

The analysis of the column charts show that the coefficients v_L, v_R significantly affect the presumed certainty. When $v_L=v_R=1.0$, *3-5* units of time are enough to obtain complete uncertainty in the previously obtained data. On the other hand, when $v_L=v_R=0.01$ (Figure 6.g), the data practically does not age over time, which is very dangerous for decision-making in a dynamic environment, when the situation changes over time. This is consistent with the data of cognitive sciences [26]. The analysis of column charts in the presence of data on the dynamic characteristics of the environment allows to choose the values of the coefficients of the aging rate in such a way as to minimize the risks of AIUS when making decisions [27].

5. Conclusion

FAI, as a blueprint of AI of the new generation, is intended to ensure the autonomy of the operation of the third generation AIUS. Along with other cognitive functions, FAI embodies such a function as the reception of data from sensors. The CP model considered in the paper takes into account such cognitive processes as the mapping of sensory information in iconic memory and its further processing in short-term memory by generalizing and abstracting data from sensors. An important feature of cognitive perception is permanent forgetting over time due to the aging of information stored in short-term memory. The listed cognitive processes are embodied in the CP model in the form of models of EMKG and IMKG, which are based, in turn, on the model of the fuzzy CF. Conducted computer experiments with the CP model confirmed the functionality of the data aging mechanism and its impact on the confidence of decision-making in AIUS. It is shown, firstly, that the CP model distills the meaning of data from sensors and represents it at a high level of abstraction, and this opens up the possibility of using FLS as a decision-making and control mechanism in AIUS. Secondly, the CP model, due to the substantial reduction in the size of the FLS decision-making space, also solves the problem of large computing resources, which is important for real-time processing. Thirdly, setting the time parameters of the CP model, namely t, v_L, v_R to the dynamic characteristics of the environment, significantly affects the increase in the level of autonomy. With small values of $v_L=v_R\approx0$, AIUS's knowledge of its environment does not age over time, which is very dangerous for decision-making in a dynamic environment in conditions of limited information, and conversely, with large values of $v_L=v_R\approx1$, knowledge is quickly forgotten. With the availability of data on the dynamic characteristics of the environment, it becomes possible to choose the values of the aging rate coefficients in such a way as to minimize AIUS risks when making decisions. Computer modeling and experiments with the AIUS prototype confirm the possibility of using the CP model as a base component of FAI supported AIUS autonomy, which opens up possibilities for further development of this direction.

In the future, it is planned to develop a FAI learning model in operational mode with the aim of automatically tuning the time parameters of the CP model to the dynamic properties of the AIUS environment.

6. References

[1] H. Shakhatreh et al., Unmanned Aerial Vehicles (UAVs): A Survey on Civil Applications and Key Research Challenges, J. IEEE Access, 7 (2019) 572–634. doi:10.1109/ACCESS.2019.2909530S.

[2] Unmanned Systems. NovAtel, 2022. URL: https://novatel.com/industries/unmanned-systems.

[3] The Future of Autonomy. Isn't Human-Less. It's Human More. Lockheed Martin, 2022. URL: https://www.lockheedmartin.com/en-us/capabilities/autonomous-unmanned-systems.html.

[4] S. Rasmussen, D. Kingston, L. Humphrey, Brief Introduction to Unmanned Systems Autonomy Services (UxAS), in: Proceedings of the 2022 Int. Conf. on Unmanned Aircraft Syst. (ICUAS), Jun 2018, 2018, pp. 257-268. doi:10.1109/ICUAS.2018.8453287.

[5] T. A. Litman, Autonomous Vehicle Implementation Predictions: Implications for Transport Planning, Victoria Transport Policy Inst., Rep., Aug, 2022.

[6] T. Zhang et al., Current trends in the development of intelligent unmanned autonomous systems, Frontiers Inf. Technol. Electron. Eng., 18 (2017) 68–85. doi:10.1631/FITEE.1601650.

[7] A. Kargin, T. Petrenko, Feeling Artificial Intelligence for AI-Enabled Autonomous Systems, in: Conference Proceedings of 2022 IEEE Global Conference on Artificial Intelligence and Internet of Things (GCAIoT), Alamein New City, Egypt, 18-21 December 2022, 2022, pp.88-93.
[8] J. Chen, J. Sun, G. Wang, From Unmanned Systems to Autonomous Intelligent Systems, Engineering, 12 (2022) 16-19. doi: 10.1016/j.eng.2021.10.007.
[9] J. Reis, Y. Cohen, N. Melao, J. Costa, D. Jorge, High-Tech Defense Industries: Developing Autonomous Intelligent Systems, Appl. Sci., 11 (2021). doi:10.3390/app11114920.
[10] M. Huang, R. Rust, Artificial Intelligence in Service, J. of Service Res., 21 2 (2018) 155-172. doi:10.1177/1094670517752459.
[11] M. Czerwinski, J. Hernandez, D. Mcduff, Building an AI That Feels: AI systems with emotional intelligence could learn faster and be more helpful, IEEE Spectrum, 58 5 (2021) 32-38. doi:10.1109/MSPEC.2021.9423818.
[12] A. Kargin, T. Petrenko, Knowledge Distillation for Autonomous Intelligent Unmanned System, in: Witold Pedrycz, Shyi-Ming Chen, Advancements in Knowledge Distillation: Towards New Horizons of Intelligent Systems, Studies in Computational Intelligence, Springer International Publishing, 1100, 2023, pp. 193-231.
[13] G. Garcia, J. Luengo, F. Herrera, Data preprocessing in data mining, Intelligent Systems Reference Library, Springer, Cham, 2015. doi:10.1007/978-3-319-10247-4.
[14] A.U. Hag, G. Zhang, H. Peng, S.U. Rahman, Combining Multiple Feature-Ranking Techniques and Clustering of Variables for Feature Selection, IEEE Access 7, 2019, pp. 151482-151492. doi:10.1109/ACCESS.2019.2947701.
[15] P. West et al., Symbolic Knowledge Distillation: from General Language Models to Commonsense Models, 2022. doi:10.48550/arXiv.2110.07178.
[16] M. Negnevitsky, Artificial Intelligence: A Guide to Intelligent Systems, 2nd ed, Addison-Wesley, 2005, 415 p.
[17] A. Kargin, T. Petrenko, Knowledge Representation in Smart Rules Engine, 3rd IEEE International Conference on Advanced Information and Communication Technologies (AICT 2019), 2019, pp. 231-236. doi:10.1109/aiact.2019.8847831.
[18] L.A. Zadeh, Computing with words. Principal concepts and ideas, Studies in Fuzziness and Soft Computing 277, Springer, Berlin, 2012. doi:10.1007/978-3-642-27473-2.
[19] A. Kargin, T. Petrenko, Spatio-Temporal Data Interpretation Based on Perceptional Model, in: Advances in Spatio-Temporal Segmentation of Visual Data, Studies in Computational Intelligence, V. Mashtalir, I. Ruban, V. Levashenko (Eds.), Springer, Cham, vol. 876, 2020, pp. 101-159. doi:10.1007/978-3-030-35480-0_3.
[20] L.A. Zadeh, Toward a Restriction-Centered Theory of Truth and Meaning (RCT), in: L. Magdalena, J. Verdegay, F. Esteva (Eds.) Enric Trillas: A Passion for FSs, A Collection of Recent Works on Fuzzy Logic, Studies in Fuzziness and Soft Computing, Springer, Cham, vol. 322, 2015, pp.1-22. doi:10.1007/978-3-319-16235-5_1.
[21] End-to-End Automation with Intelligent and Integrated Robotic Solutions. 2023. URL: https://www.primerobotics.com/robots/.
[22] P. Ramamurthy, S.N. Aakur, ISD-QA: Iterative Distillation of Commonsense Knowledge from General Language Models for Unsupervised Question Answering, in: 26th International Conference on Pattern Recognition (ICPR), 2022, pp.1229-1235. doi:10.1109/ICPR56361.2022.9956441.
[23] J. Bach, Principles of Synthetic Intelligence: Psi: An Architecture of Motivated Cognition, 1st. ed. Oxford University Press, New York, 2009.
[24] A. Piegat, Fuzzy modelling and control, Heidelberg: Physica-Verlag Heidelberg, New York, 2001.
[25] A. Kaufmann, Introduction to the theory of fuzzy subsets, 1st. ed, Academic Pr., 1975.
[26] R.M. Shiffrin, Short-term store: The basis for a memory system, in: Cognitive theory, F. Restle, R. M. Shiffrin, N. J. Castellan, H.R. Lindman, D. B. Pisoni (Eds.), vol.1, Hillsdale, NJ: Erlbaum., 2018, pp. 193-218. doi:10.4324/9780203781548-13.
[27] A. Kargin, T. Petrenko, Method of Using Data from Intelligent Machine Short-Term Memory in Fuzzy Logic System, in: Conf. Proc. of 2021 IEEE 7th World Forum on Internet of Things (WF-IoT), New Orleans, Louisiana, USA, 20-24 June 2021, 2021, pp. 842-847. doi:10.1109/aiact.2019.8847831.